

StableWorld: Towards Stable and Consistent Long Interactive Video Generation

Ying Yang¹, Zhengyao Lv^{1,2}, Tianlin Pan^{1,3}, Haofan Wang⁴, Binxin Yang⁵,
Hubery Yin⁵, Chen Li⁵, Ziwei Liu⁶, Chenyang Si^{1†},

¹PRLab, NJU ²HKU ³UCAS ⁴LibLib.ai ⁵WeChat, Tencent Inc. ⁶NTU

<https://sd-world.github.io/>



Figure 1. **StableWorld**: producing stable and visually consistent interactive videos across diverse environments such as natural landscapes and game worlds, while preserving continuous motion control and preventing long-term scene drift.

Abstract

In this paper, we explore the overlooked challenge of stability and temporal consistency in interactive video generation, which synthesizes dynamic and controllable video worlds through interactive behaviors such as camera movements and text prompts. Despite remarkable progress in world modeling, current methods still suffer from severe instability and temporal degradation, often leading to spatial drift and scene collapse during long-horizon interactions. To better understand this issue, we initially investigate the underlying causes of instability and identify that the major source of error accumulation originates from the same

scene, where generated frames gradually deviate from the initial clean state and propagate errors to subsequent frames. Building upon this observation, we propose a simple yet effective method, **StableWorld**, a Dynamic Frame Eviction Mechanism. By continuously filtering out degraded frames while retaining geometrically consistent ones, **StableWorld** effectively prevents cumulative drift at its source, leading to more stable and temporal consistency of interactive generation. Promising results on multiple interactive video models, e.g., *Matrix-Game*, *Open-Oasis*, and *Hunyuan-GameCraft*, demonstrate that **StableWorld** is model-agnostic and can be applied to different interactive video generation frameworks to substantially improve stability, temporal consistency, and generalization across diverse interactive scenarios.

† Corresponding Author.

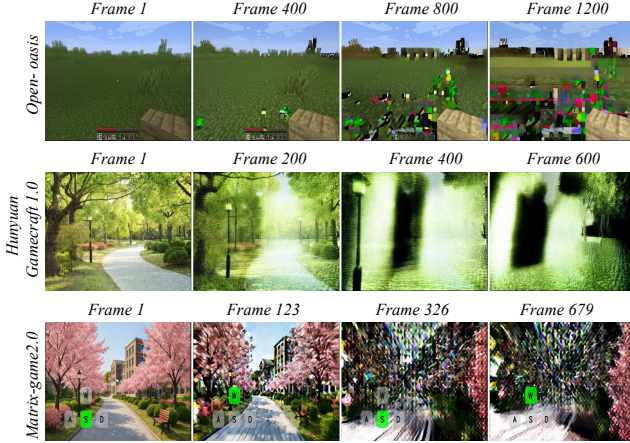


Figure 2. Visualization of progressive scene collapse over time across different world-simulation models.

1. Introduction

Recent advances in video generation [20, 32, 34, 36] have achieved remarkable success in learning rich spatio-temporal knowledge from large-scale videos. Building upon these capabilities, recent studies [4, 7, 9, 10, 12, 21, 25, 37, 41, 45] have leveraged video generation models to understand real-world interactions and predict environment dynamics conditioned on actions, extending them toward the paradigm of world modeling. However, as shown in Fig. 2, current world models commonly suffer from a phenomenon of progressive scene collapse as time elapses, particularly in static or slowly changing environments. Hence, ensuring long-term stability and temporal consistency across diverse actions and scenes, especially in generating long interactive videos without scene collapse, remains a fundamental yet insufficiently explored challenge in world modeling.

In this paper, we delve into the phenomenon of degradation in world models. For a comprehensive analysis, we begin with the simplest form of interaction, *i.e.* static interaction, by generating long static video sequences to observe how scene stability evolves over time. To this end, we measure inter-frame mean squared error (MSE) distances to quantify how frame discrepancies accumulate as the sequence progresses. As illustrated in Fig. 3, while consecutive frames differ only slightly, these subtle deviations accumulate over time, leading to a noticeable drift from the initial clean state. As the drift accumulates over time, it manifests as visible inconsistencies and eventually leads to progressive scene collapse. These observations suggest that error accumulation within the same scene, even under minimal interaction, is a key factor contributing to instability in current world models.

Based on this observation, we hypothesize that using frames with smaller accumulated drift as historical refer-

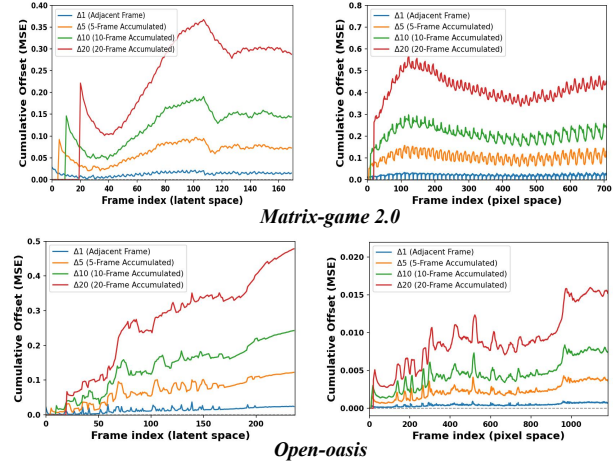


Figure 3. Accumulated frame-to-frame drift in **Matrix-Game 2.0** and **Open-Oasis**.

ences can provide a more stable foundation for subsequent frame generation. To verify this hypothesis, we analyze the impact of enlarging the KV-cache window size, which allows the model to access earlier and potentially cleaner frames during generation. As shown in Fig. 4, increasing the window size effectively mitigates the degradation phenomenon by reducing frequency amplitude fluctuations between each target frame and the first frame. This finding suggests that incorporating temporally cleaner frames can suppress cumulative errors and stabilize long-horizon generation. Further analysis reveals that the observed stabilization when enlarging the history window primarily arises from retaining several clean early frames within the reference buffer.

With these revelations as our backdrop, we introduce **StableWorld**, a simple yet effective framework for building an interactive world model capable of generating stable and temporally consistent videos, as shown in Fig. 5. The core design of StableWorld is Dynamic Frame Eviction Mechanism to dynamically maintain a clean and reliable historical frame representations in the sliding window for current-frame generation. When the window needs to slide as new frames are appended, some historical frames must be evicted. We always retain the most recent frames, since they are critical for preserving local motion continuity and visual smoothness. For earlier frames, we designate the earliest, least-degraded frames in the window as the reference frames, and evaluate geometric consistency between it and intermediate frames using a viewpoint-overlap score computed via ORB + RANSAC [8, 28]. If multiple intermediate frames share a similar viewpoint with the reference, they are regarded as redundant and potentially drifted, and are selectively evicted to prevent further error accumulation. **By continuously filtering out degraded frames while retaining geometrically consistent ones**, StableWorld effectively

suppresses cumulative errors while preserving adaptability to large motions and scene transitions, enabling stable and consistent interactive video generation.

We conduct a comprehensive experimental evaluation of our approach. The results demonstrate that **StableWorld** significantly reduces cumulative drift while maintaining motion continuity across diverse scenarios, as shown in Fig. 1. Our contributions are summarized as follows:

- We identify the root cause of instability in long interactive world modeling: small drifts accumulate within the same scene, eventually leading to overall scene collapse.
- We propose a simple yet effective method **StableWorld**, a dynamic frame eviction mechanism that effectively prevents error accumulation at its source while maintaining motion continuity.
- We validate our method across multiple interactive world models—Matrix-Game 2.0, Open Oasis, and Hunyuan-GameCraft 1.0—under diverse conditions (static scenes, small/large motions, and significant viewpoint changes). Extensive results show consistent improvements in stability, long-term consistency, and generalization across various interactive scenarios.

2. Related work

Video Generation Models. With the rapid development of diffusion models [2, 14, 15, 26, 27, 29], video generation has also made remarkable progress in producing high-quality and temporally coherent videos [1, 3, 16, 20, 22, 34, 36, 39, 44, 46]. These methods typically extend image diffusion into the spatiotemporal domain, enabling globally consistent visual appearance across multiple frames. Meanwhile, autoregressive models have achieved significant advances in both image [11, 30, 33, 43, 47] and video generation [6, 13, 17, 19, 23, 24, 32, 35, 40] due to their strong scalability and controllability. By generating videos in a step-by-step manner conditioned on previously produced tokens, autoregressive models naturally support long-horizon temporal modeling and interactive generation.

Interactive World Simulation. Generating interactive environments can be regarded as a form of world simulation, often referred to as *world models* [4, 10, 25], which predict the next state in an autoregressive manner conditioned on the current state and action. Recently, the emergence of high-quality world models built upon powerful video generation techniques has led to rapid progress [7, 9, 12, 21, 38, 42, 45]. Some studies [7, 9, 21] focus on improving action following and maintaining temporal continuity, while others [37, 41] aim to enhance memory consistency to ensure that the scene remains coherent under the same viewpoint across subsequent generations. These efforts collectively improve interactive controllability and short-term coherence in dynamic environments.

Long Video Generation. While recent video generation models have achieved impressive visual quality, they still struggle to produce long videos, typically limited to around 5 seconds [1, 20, 34, 39], due to prohibitive computational costs and cumulative drift. A variety of approaches have been proposed for extending long-context generation. Methods such as [21, 31] generate videos chunk by chunk, where each new segment is conditioned on the previously generated one. Although this strategy enables longer temporal horizons, it introduces high training cost and often causes motion discontinuities at chunk boundaries. Frame-packing [44] produces keyframes across different stages and interpolates intermediate frames accordingly. While this constrains error propagation between adjacent keyframes, it inevitably limits motion flexibility and generative diversity. Other approaches, including diffusion forcing [5] and self-forcing [17], simulate autoregressive degradation patterns during training to reduce the train-inference distribution gap and improve long-term temporal stability. However, these methods still suffer from error accumulation during inference. Moreover, these approaches remain largely confined to conventional Text-to-Video (T2V) or Image-to-Video (I2V) settings, leaving long interactive video generation insufficiently addressed.

3. Methodology

3.1. Preliminary

Video Generation Models. Video generation models typically adopt a *full-sequence* generation approach, which generates all frames at once from noise under a given condition c . Formally, the generation process can be defined as:

$$p_\theta(\mathbf{x}_k^t \mid \mathbf{x}_k^{t+1}, \mathbf{c}) = \mathcal{N}(\mathbf{x}_k^t; \mu_\theta(\mathbf{x}_k^{t+1}, \mathbf{c}, t), \sigma_t^2 \mathbf{I}), \quad (1)$$

where \mathbf{x}_k^t denotes the t -th denoising step of the k -th frame, and $0 \leq k \leq K$ with K being the total number of generated frames. All frames share the same noise variance σ_t at each timestep t , following a unified noise schedule. Although this approach achieves high-quality results, modeling the entire sequence in a single forward pass incurs a high computational cost and is not suitable for real-time interactive scenarios.

Interactive Video Generation. In contrast to full-sequence models, interactive video generation adopts an autoregressive paradigm, where each frame \mathbf{x}_k is generated conditioned on a subset of historical frames and the current action a_k . This conditional generation is expressed as $p_\theta(\mathbf{x}_k \mid \mathbf{x}_{\{1:k-1\}}^{\text{subset}}, a_k)$, where $\mathbf{x}_{\{1:k-1\}}^{\text{subset}}$ denotes the selected reference frames maintained in the memory buffer, and a_k represents the user-issued or agent-driven action at step k . This paradigm allows the model to generate frames sequentially in response to user actions, enabling real-time interaction and dynamic scene control.

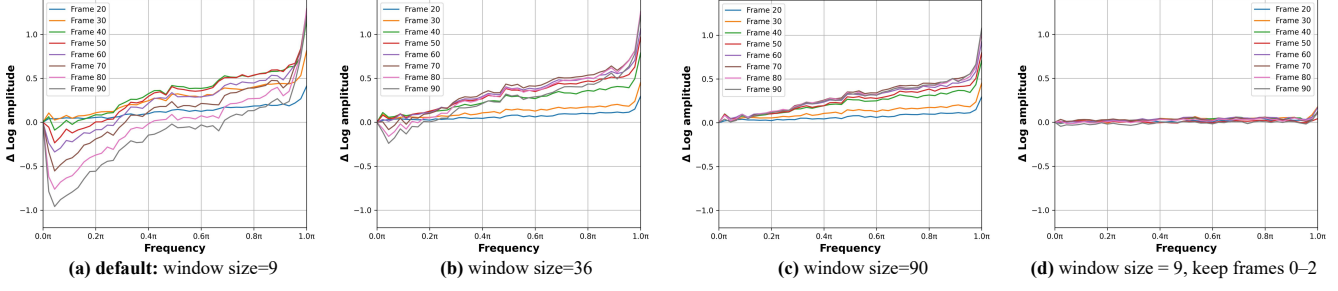


Figure 4. Frequency amplitude difference between the anchor frame and different target frames. (a) Default setting: window size = 9. (b) window size = 36. (c) window size = 90. (d) window size = 9 with the first clean 3 frames retained.

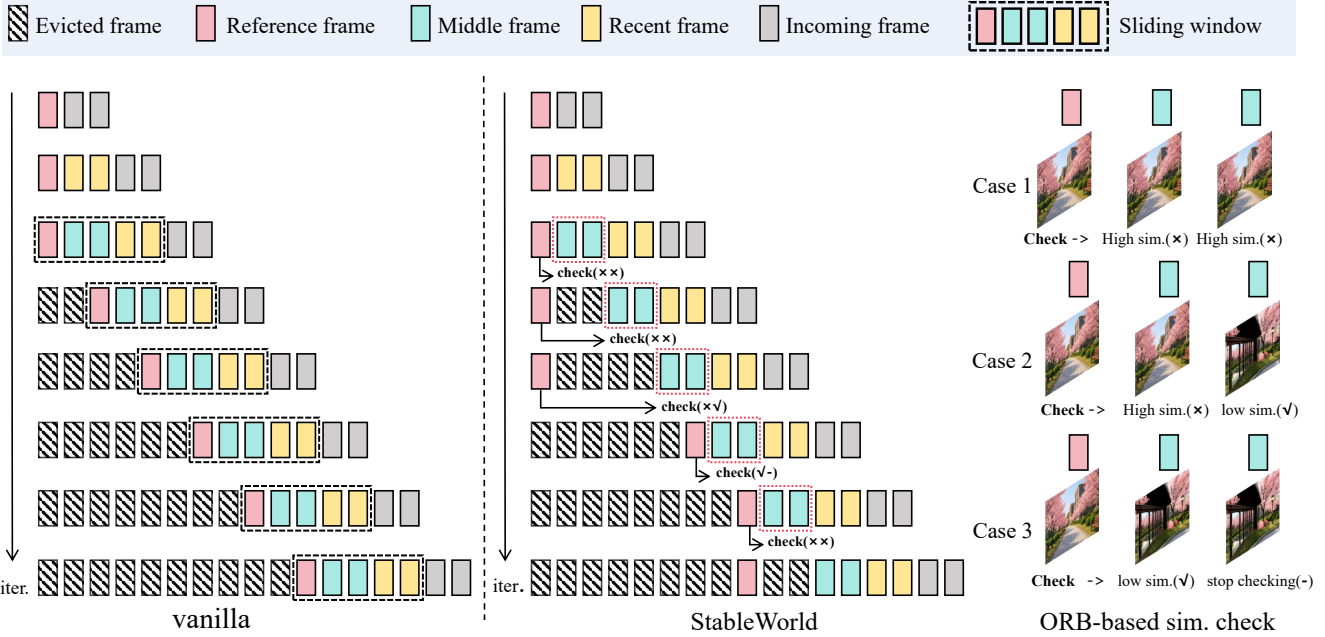


Figure 5. Comparison of sliding-window updates. When the window slides, the vanilla model simply discards the oldest frames, causing errors to accumulate over iterations. In contrast, **StableWorld** continuously filters out degraded frames while maintaining geometrically consistent ones, resulting in more stable and consistent interactive video generation.

Most recent approaches further combine diffusion and autoregressive paradigms: diffusion models are used for *intra-frame* denoising, while autoregression captures *inter-frame* temporal dependencies. Formally, the overall generation process can be expressed as:

$$\begin{aligned} p_{\theta}(\mathbf{x}_k^t | \mathbf{x}_k^{t-1}, \mathbf{x}_{\{1:k-1\}}^{\text{subset}}, a_k) \\ = \mathcal{N}(\mathbf{x}_k^t; \mu_{\theta}(\mathbf{x}_k^{t-1}, \mathbf{x}_{\{1:k-1\}}^{\text{subset}}, a_k, t), \sigma_t^2 \mathbf{I}), \end{aligned} \quad (2)$$

where \mathbf{x}_k^t denotes the k -th frame at diffusion timestep t . At each diffusion step t , the model denoises \mathbf{x}_k^{t-1} into \mathbf{x}_k^t conditioned on previously generated frames $\mathbf{x}_{\{1:k-1\}}^{\text{subset}}$ and the current action a_k . This formulation integrates spatial denoising within each frame and temporal dependencies across frames, enabling high-quality and real-time interactive video

generation.

3.2. The Reason for Scene Collapse

Although interactive video generation models can produce coherent short-term sequences, they still tend to exhibit progressive *scene collapse* during long-duration generation, particularly when the scene remains highly similar for an extended period (Fig. 2). In contrast, this collapse rarely occurs when scene transitions happen frequently, where the model continuously encounters new visual conditions (Fig. 6). This contrast suggests that the collapse is, to a large extent, not caused by action control or motion complexity, but is instead related to how visual information is preserved and propagated within the same scene over time.

To understand this behavior, we measure the inter-frame



Figure 6. No scene collapse occurs in the vanilla model under frequent scene switching.



Figure 7. Comparison under scene switching settings. The first row shows the vanilla model, while the second row keeps the first three frames unchanged.

mean squared error (MSE) distances to quantify how frame discrepancies change as the sequence progresses within a single static scene, as shown in Fig. 3. The left two plots visualize inter-frame drift at different intervals (1, 5, 10, 20) in the latent space. We observe that although adjacent frames exhibit only minor discrepancies, these small drifts gradually accumulate as the sequence extends. Frames compared over larger intervals (e.g., 10 or 20) show significantly greater drift. Since such deviations are already present in the latent space, the pixel space also exhibits a similar drift pattern, as shown in the right two plots, which ultimately manifests as visual inconsistency and scene collapse (see Fig. 2). These observations demonstrate that **drift within a single scene accumulates and propagates over time, ultimately leading to global scene collapse**.

Based on this observation, we hypothesize that using frames with smaller accumulated drift can provide more reliable references for subsequent frame generation. To verify this hypothesis, we enlarge the KV-cache window size, allowing the model to access cleaner frames, as shown in Fig. 4. We examine how the frequency amplitude difference between each target frame and the first frame varies under different history window sizes. With the default setting (window size = 9, panel (a)), large variations appear across all frequency bands. As the window size increases to 36 (panel (b)) and 90 (panel (c)), the overall fluctuation slows down, indicating a partial reduction of error accumulation. However, this improvement comes at the cost of higher computational overhead and slower generation, which limits its practicality.

Further analysis reveals that the observed stabilization from a larger window primarily arises from retaining sev-

eral clean early frames in the reference buffer. For example, in panel (d), preserving a few reliable early frames within a fixed-size window leads to notably more stable generation, with later frames showing minimal drift relative to the first frame. This finding highlights that **the quality and preservation of early clean frames play a crucial role in mitigating cumulative errors**. Nevertheless, when large motions or drastic scene transitions occur, always retaining the initial frames becomes restrictive. As shown in Fig. 7, although both settings follow the same action instructions, the one that rigidly preserves early frames fails to switch to a new scene, suggesting that excessive retention hinders scene transitions. To simultaneously mitigate cumulative drift and preserve the flexibility to generate new scenes, we introduce **StableWorld**, a simple yet effective framework built upon a *Dynamic Frame Eviction Mechanism* (see Fig. 5), which will be described in the following section.

3.3. Dynamic Frame Eviction via ORB-based Geometric Similarity

To determine whether a scene transition occurs, we employ ORB [28] feature matching combined with RANSAC-based geometric verification to measure inter-frame similarity. When there aren't explicit camera extrinsic parameters in the inference stage, ORB provides an alternative that can produce fast and rotation-invariant local features, making it well-suited for detecting geometric consistency under small camera motions. By integrating this similarity estimation with a dynamic frame eviction strategy, we **continuously filter out degraded frames while retaining geometrically consistent ones**, thereby effectively preventing error accumulation across dynamic scenes.

Specifically, when the window needs to slide, some frames must be evicted. For simplicity, we assume that each frame corresponds to one token, and one token is generated at each iteration. Let $\{L_0, L_1, \dots, L_{N-1}\}$ denote the latent-space tokens within the window, and $\{P_0, P_1, \dots, P_{N-1}\}$ denote their corresponding pixel-space frames, where N is the window size. The earlier frames in the window are defined as $\{P_0, P_1, \dots, P_K\}$ with $K < N - 1$. Here, P_0 is treated as the reference frame, while $\{P_1, \dots, P_K\}$ are referred to as the middle frames. At each update step, one new frame is generated, and one old frame is evicted accordingly.

We determine which frame should be evicted using the following strategy. First, we measure geometric similarity by extracting ORB features from the reference frame P_0 and a middle frame P_k ($k \geq 1$). Let $\{\mathbf{d}_i^{(0)}\}_{i=1}^{M_0}$ and $\{\mathbf{d}_j^{(k)}\}_{j=1}^{M_k}$ denote the sets of ORB descriptors extracted from P_0 and P_k , respectively, where M_0 and M_k are the numbers of detected features in each frame. Candidate correspondences G are obtained by nearest-neighbor matching in descriptor space, followed by Lowe's ratio test:

$$G = \{(i, j) \mid \|\mathbf{d}_i^{(0)} - \mathbf{d}_j^{(k)}\| < \tau\}, \quad g = |G|, \quad (3)$$

where τ is the ratio-test threshold used to filter ambiguous matches, and $g = |G|$ denotes the number of surviving correspondences.

The matches in G are then verified using RANSAC with both Homography (\mathbf{H}) and Fundamental matrix (\mathbf{F}) models to enforce geometric consistency:

$$\mathcal{I}_H = \{(i, j) \in G \mid \text{SampsonErr}_{\mathbf{H}}(i, j) \leq \epsilon\}, \quad (4)$$

$$\mathcal{I}_F = \{(i, j) \in G \mid \text{SampsonErr}_{\mathbf{F}}(i, j) \leq \epsilon\}, \quad (5)$$

where $\text{SampsonErr}_{\mathbf{H}}(i, j)$ and $\text{SampsonErr}_{\mathbf{F}}(i, j)$ denote the Sampson geometric errors evaluated under the estimated Homography \mathbf{H} and Fundamental matrix \mathbf{F} , respectively, and \mathcal{I}_H and \mathcal{I}_F denote the corresponding inlier correspondence sets. ϵ is a predefined tolerance for inlier determination, with smaller errors indicating better geometric alignment. We compute the inlier ratios:

$$r_H = \frac{|\mathcal{I}_H|}{g}, \quad r_F = \frac{|\mathcal{I}_F|}{g}, \quad (6)$$

where $|\mathcal{I}_H|$ and $|\mathcal{I}_F|$ denote the numbers of inlier correspondences under the two models. The final similarity score is defined as:

$$s(P_0, P_k) = \max(r_H, r_F). \quad (7)$$

If the similarity score $s(P_0, P_k)$ exceeds a predefined threshold θ , the check continues iteratively for farther frames (P_{k+1}, P_{k+2}, \dots). The process stops once geometric similarity drops below θ . Finally, if all middle frames satisfy the threshold, the farthest frame P_K is evicted. Otherwise, the frame directly preceding the first failure (e.g., P_{k-1}) is evicted. The detailed procedure and implementation settings are provided in Appendix A.

4. Experiments

4.1. Evaluation Metrics.

To evaluate the effectiveness of our proposed method compared to the baseline, we conduct both qualitative and quantitative experiments across multiple models and scenarios. For *Matrix-Game 2.0* [12], we evaluate 16 different scenes, covering various environments as well as small and large motion actions, resulting in a total of 80 one-minute videos. For *Open-Oasis* [7], we evaluate 10 different scenes and generate 50 one-minute videos involving diverse motions. For *Hunyuan-GameCraft 1.0* [21], we evaluate 16 scenes and generate 48 videos, each lasting 45 seconds. We use the VBench-Long [18] benchmark to assess multiple dimensions of video quality and consistency. Further, we also conduct a user study with 20 participants to assess the video quality, temporal consistency, and the motion smoothness in 30 videos of the three models. In addition, we also verify the effectiveness of *StableWorld* as an error mitigation strategy in autoregressive video generation, evaluated under the **Self-Forcing** [17] (see Appendix D).

4.2. Implementation Details

For *Matrix-Game 2.0*, we set the key-value cache length to 9 and treat the earliest 6 frames as earlier frames. Since the model generates 3 frames at each step, we compute the ORB-based similarity for the 3rd and 6th frames to determine which frames to evict. For *Open-Oasis*, the model generates one frame per step with a default window size of 16. We designate the earliest 12 frames in the window as earlier frames and evaluate ORB-based similarity for the 1st, 6th, and 12th frames. For *Hunyuan-GameCraft 1.0*, the model generates 33 frames at each step, where the newly generated 33 frames form the new window. We compare the 1st, 6th, and 12th frames of the previous window with their corresponding frames in the new window. If the similarity is above the threshold, the earlier frames are merged into the new window. For all models, we set the ORB-based similarity threshold to 0.75. Some experiments are run on Ascend 910B2.

4.3. Quantitative Results

VBench-Long Metrics. Tab. 1 compares the VBench-Long scores between the vanilla models and our *StableWorld*-enhanced versions across three settings. We observe significant improvements in both *Image Quality* and *Aesthetic Quality*. For example, on *Matrix-Game 2.0*, *StableWorld* improves the Aesthetic Quality score by 14.61%; on *Open-Oasis*, it improves the Image Quality score by 7.38%; and on *Hunyuan-GameCraft 1.0*, it boosts the Aesthetic Quality by 9.06%. Meanwhile, we note that the *Temporal Quality* and *Physical Understanding* metrics do not show large differences between the vanilla models and *StableWorld*. This is because once collapse occurs, the vanilla model tends to produce visually similar and nearly static subjects, which inadvertently stabilizes these metrics. Nevertheless, *StableWorld* consistently achieves improvements on most metrics, indicating that it alleviates error accumulation while better preserving subject identity and motion continuity. Our method introduces only minimal additional computational overhead (1.00–1.02×).

User Study. Tab. 2 shows that *StableWorld* receives the majority of votes, further confirming the substantial improvements in visual quality, temporal consistency, and motion smoothness achieved by *StableWorld*.

4.4. Qualitative Results

Fig. 8 visualizes qualitative results from all three models, showing that *StableWorld* maintains better scene stability and reduces drift over time. Additional qualitative comparisons are provided in Appendix C. We further compare autoregressive video generation with Self-Forcing and our proposed method in Appendix D. These results demonstrate the generalizability and effectiveness of *StableWorld*, which significantly alleviates error accumulation at its source by

Table 1. Quantitative comparison on VBench-Long [18] across three vanilla models and their StableWorld-enhanced counterparts. Our StableWorld method improves both visual and temporal quality with minimal additional latency.

Method	Latency	Visual Quality			Temporal Quality		Physical Understanding	
		Image Quality \uparrow	Aesthetic \uparrow	Dynamic Degree \uparrow	Temporal Flickering \uparrow	Motion Smooth \uparrow	Subject Cons. \uparrow	Background Cons. \uparrow
Matrix-Game 2.0	$\times 1.00$	63.39	38.83	56.19	95.19	97.41	96.49	97.52
StableWorld + Matrix-Game 2.0	$\times 1.01$	73.52	53.44	56.66	95.96	98.13	97.02	97.74
Open-Oasis	$\times 1.00$	66.37	43.80	16.81	99.53	99.52	98.94	99.18
StableWorld + Open-Oasis	$\times 1.02$	73.75	48.73	20.04	99.67	99.62	98.84	99.52
Hunyuan-GameCraft 1.0	$\times 1.00$	57.91	48.38	98.00	95.66	98.27	97.21	96.83
StableWorld + Hunyuan-GameCraft 1.0	$\times 1.02$	65.91	57.44	98.66	96.05	98.29	97.08	97.06



Figure 8. Qualitative comparison between baseline results and our proposed *StableWorld* across three models. Each pair of rows corresponds to one model: (1) *Matrix-Game 2.0*, (2) *Open-Oasis*, and (3) *Hunyuan-GameCraft 1.0*. In each group, the first row shows the baseline results and the second row shows our *StableWorld* outputs, which maintain higher scene stability, smoother motion, and more consistent temporal dynamics.

Table 2. User study comparing three vanilla models and their StableWorld-enhanced counterparts across three criteria. Values denote the percentage of users preferring the method.

Model	Video Qual. \uparrow	Temporal Cons. \uparrow	Motion Smo. \uparrow
Matrix-Game 2.0	23.2%	12.5%	14.3%
StableWorld + Matrix.	76.8%	87.5%	85.7%
Open-Oasis	3.6%	5.4%	7.1%
StableWorld + Open.	96.4%	94.6%	92.9%
Hunyuan-GameCraft 1.0	10.7%	3.6%	7.1%
StableWorld + Hunyuan.	89.3%	96.4%	92.9%

continuously filtering out degraded frames across different scenes.

4.5. Ablation Studies

Different Window Sizes We compare different window sizes in Fig. 9 using the *Matrix-Game 2.0 + StableWorld*.

All settings share the same action conditions. As the window size increases, the generation of subsequent scenes becomes affected. When the window size is set to 18 or 36, too many historical frames introduce residual artifacts from old scenes into new ones, which eventually interfere with the generation of new scenes, particularly evident when the window size reaches 36.

Different Similarity Metrics. We further compare different similarity metrics, including SSIM and cosine similarity, as shown in Fig. 11. The SSIM threshold is set to 0.3, and the cosine similarity threshold is set to 0.8. SSIM is overly sensitive to geometric perspective changes, while cosine similarity is less sensitive to spatial transformations, as also shown in Fig. 10. As a result, cosine-based similarity sometimes fails to detect scene changes, causing frames from old scenes to remain in the window, which leads to visible artifacts in the new scene. In contrast, SSIM tends to evict



Figure 9. Comparison of *StableWorld* under different window sizes.

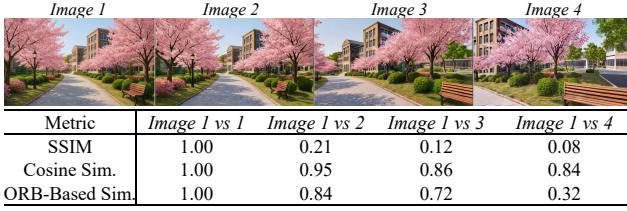


Figure 10. Comparison of different similarity metrics used for frame evaluation.

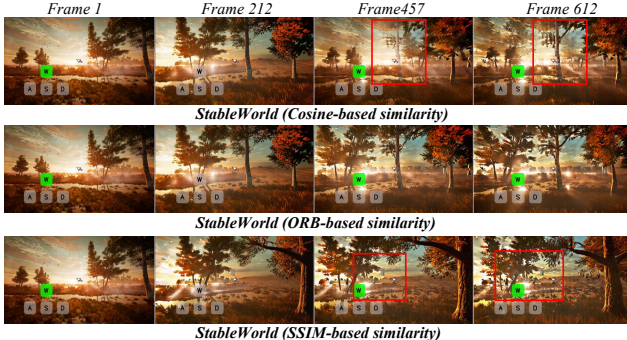


Figure 11. *StableWorld* results under different similarity metrics: Cosine-based similarity, ORB-based similarity and SSIM-based similarity.

clean frames too early, resulting in more severe cumulative errors compared to other metrics.

Different ORB-Based Similarity Threshold. We further evaluate the impact of different ORB-based similarity thresholds (0.35, 0.55, 0.75, 0.95) in Fig. 12. A lower threshold (e.g., 0.35) retains old frames for too long, hindering the generation of new scenes. Similarly, a threshold of 0.55 still causes noticeable interference between adjacent scenes. In contrast, a very high threshold (e.g., 0.95) leads to the premature eviction of clean frames, introducing mild cumu-

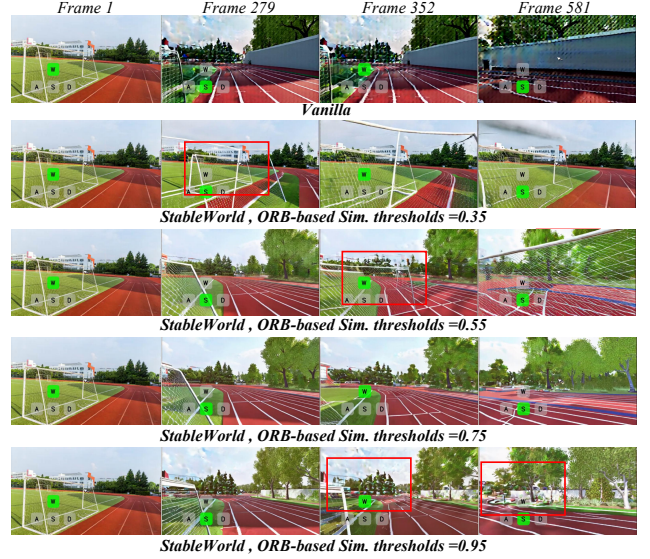


Figure 12. *StableWorld* under different ORB-based similarity thresholds. The figure shows how varying the threshold affects frame eviction behavior and overall scene stability.

lative errors. Overall, the threshold of 0.75 achieves the best trade-off, effectively reducing error accumulation without compromising motion consistency.

5. Conclusion

In this paper, we identify a common problem faced by current interactive video generation models: *scene collapse*. Through further analysis, we find that this collapse originates from the inter-frame drift that occurs between adjacent frames within the same scene, which gradually accumulates over time and eventually leads to a large deviation from the original scene. Motivated by this observation, we propose a simple yet effective method — **StableWorld**, a dynamic frame eviction mechanism that significantly reduces error accumulation while preserving motion consistency. We evaluate our approach on multiple interactive video generation models, including *Matrix-Game 2.0*, *Open-Oasis*, and *Hunyan-GameCraft 1.0*. Extensive experiments demonstrate that our method substantially improves visual quality over long horizons and shows strong potential for integration with future world models.

6. Acknowledgements

This study is supported by the Fundamental Research Funds for the Central Universities (KG2025XX). This research is also supported by cash and in-kind funding from industry partner(s).

References

[1] Fan Bao, Chendong Xiang, Gang Yue, Guande He, Hongzhou Zhu, Kaiwen Zheng, Min Zhao, Shilong Liu, Yaole Wang, and Jun Zhu. Vidu: a highly consistent, dynamic and skilled text-to-video generator with diffusion models. *arXiv preprint arXiv:2405.04233*, 2024. 3

[2] Stephen Batifol, Andreas Blattmann, Frederic Boesel, Saksham Consul, Cyril Diagne, Tim Dockhorn, Jack English, Zion English, Patrick Esser, Sumith Kulal, et al. Flux. 1 kontext: Flow matching for in-context image generation and editing in latent space. *arXiv e-prints*, pages arXiv–2506, 2025. 3

[3] Tim Brooks, Bill Peebles, Connor Holmes, Will DePue, Yufei Guo, Li Jing, David Schnurr, Joe Taylor, Troy Luhman, Eric Luhman, et al. Video generation models as world simulators. *OpenAI Blog*, 1(8):1, 2024. 3

[4] Jake Bruce, Michael D Dennis, Ashley Edwards, Jack Parker-Holder, Yuge Shi, Edward Hughes, Matthew Lai, Aditi Mavalankar, Richie Steigerwald, Chris Apps, et al. Genie: Generative interactive environments. In *Forty-first International Conference on Machine Learning*, 2024. 2, 3

[5] Boyuan Chen, Diego Martí Monsó, Yilun Du, Max Simchowitz, Russ Tedrake, and Vincent Sitzmann. Diffusion forcing: Next-token prediction meets full-sequence diffusion. *Advances in Neural Information Processing Systems*, 37:24081–24125, 2024. 3

[6] Justin Cui, Jie Wu, Ming Li, Tao Yang, Xiaojie Li, Rui Wang, Andrew Bai, Yuanhao Ban, and Cho-Jui Hsieh. Self-forcing++: Towards minute-scale high-quality video generation. *arXiv preprint arXiv:2510.02283*, 2025. 3

[7] Etched Decart, Quinn McIntyre, Spruce Campbell, Xinlei Chen, and Robert Wachen. Oasis: A universe in a transformer. URL: <https://oasis-model.github.io>, 2024. 2, 3, 6

[8] Martin A Fischler and Robert C Bolles. Random sample consensus: a paradigm for model fitting with applications to image analysis and automated cartography. *Communications of the ACM*, 24(6):381–395, 1981. 2

[9] Junliang Guo, Yang Ye, Tianyu He, Haoyu Wu, Yushu Jiang, Tim Pearce, and Jiang Bian. Mineworld: a real-time and open-source interactive world model on minecraft. *arXiv preprint arXiv:2504.08388*, 2025. 2, 3

[10] David Ha and Jürgen Schmidhuber. Recurrent world models facilitate policy evolution. *Advances in neural information processing systems*, 31, 2018. 2, 3

[11] Jian Han, Jinlai Liu, Yi Jiang, Bin Yan, Yuqi Zhang, Zehuan Yuan, Bingyue Peng, and Xiaobing Liu. Infinity: Scaling bitwise autoregressive modeling for high-resolution image synthesis. In *Proceedings of the Computer Vision and Pattern Recognition Conference*, pages 15733–15744, 2025. 3

[12] Xianglong He, Chunli Peng, Zexiang Liu, Boyang Wang, Yifan Zhang, Qi Cui, Fei Kang, Biao Jiang, Mengyin An, Yangyang Ren, et al. Matrix-game 2.0: An open-source, real-time, and streaming interactive world model. *arXiv preprint arXiv:2508.13009*, 2025. 2, 3, 6

[13] Roberto Henschel, Levon Khachatryan, Hayk Poghosyan, Daniil Hayrapetyan, Vahram Tadevosyan, Zhangyang Wang, Shant Navasardyan, and Humphrey Shi. Streaming2v: Consistent, dynamic, and extendable long video generation from text. In *Proceedings of the Computer Vision and Pattern Recognition Conference*, pages 2568–2577, 2025. 3

[14] Jonathan Ho and Tim Salimans. Classifier-free diffusion guidance. *arXiv preprint arXiv:2207.12598*, 2022. 3

[15] Jonathan Ho, Ajay Jain, and Pieter Abbeel. Denoising diffusion probabilistic models. *Advances in neural information processing systems*, 33:6840–6851, 2020. 3

[16] Wenyi Hong, Ming Ding, Wendi Zheng, Xinghan Liu, and Jie Tang. Cogvideo: Large-scale pretraining for text-to-video generation via transformers. *arXiv preprint arXiv:2205.15868*, 2022. 3

[17] Xun Huang, Zhengqi Li, Guande He, Mingyuan Zhou, and Eli Shechtman. Self forcing: Bridging the train-test gap in autoregressive video diffusion. *arXiv preprint arXiv:2506.08009*, 2025. 3, 6

[18] Ziqi Huang, Yinan He, Jiashuo Yu, Fan Zhang, Chenyang Si, Yuming Jiang, Yuanhan Zhang, Tianxing Wu, Qingyang Jin, Nattapol Chanpaisit, et al. Vbench: Comprehensive benchmark suite for video generative models. In *Proceedings of the IEEE/CVF Conference on Computer Vision and Pattern Recognition*, pages 21807–21818, 2024. 6, 7

[19] Yang Jin, Zhicheng Sun, Ningyuan Li, Kun Xu, Hao Jiang, Nan Zhuang, Quzhe Huang, Yang Song, Yadong Mu, and Zhouchen Lin. Pyramidal flow matching for efficient video generative modeling. *arXiv preprint arXiv:2410.05954*, 2024. 3

[20] Weijie Kong, Qi Tian, Zijian Zhang, Rox Min, Zuozhuo Dai, Jin Zhou, Jiangfeng Xiong, Xin Li, Bo Wu, Jianwei Zhang, et al. Hunyuanyvideo: A systematic framework for large video generative models. *arXiv preprint arXiv:2412.03603*, 2024. 2, 3

[21] Jiaqi Li, Junshu Tang, Zhiyong Xu, Longhuang Wu, Yuan Zhou, Shuai Shao, Tianbao Yu, Zhiguo Cao, and Qinglin Lu. Hunyuan-gamecraft: High-dynamic interactive game video generation with hybrid history condition. *arXiv preprint arXiv:2506.17201*, 2025. 2, 3, 6

[22] Bin Lin, Yunyang Ge, Xinhua Cheng, Zongjian Li, Bin Zhu, Shaodong Wang, Xianyi He, Yang Ye, Shenghai Yuan, Luhuan Chen, et al. Open-sora plan: Open-source large video generation model. *arXiv preprint arXiv:2412.00131*, 2024. 3

[23] Jinlai Liu, Jian Han, Bin Yan, Hui Wu, Fengda Zhu, Xing Wang, Yi Jiang, Bingyue Peng, and Zehuan Yuan. Infini-tystar: Unified spacetime autoregressive modeling for visual generation. *arXiv preprint arXiv:2511.04675*, 2025. 3

[24] Kunhao Liu, Wenbo Hu, Jiale Xu, Ying Shan, and Shijian Lu. Rolling forcing: Autoregressive long video diffusion in real time. *arXiv preprint arXiv:2509.25161*, 2025. 3

[25] Junhyuk Oh, Xiaoxiao Guo, Honglak Lee, Richard L Lewis, and Satinder Singh. Action-conditional video prediction using deep networks in atari games. *Advances in neural information processing systems*, 28, 2015. 2, 3

[26] William Peebles and Saining Xie. Scalable diffusion models with transformers. In *Proceedings of the IEEE/CVF international conference on computer vision*, pages 4195–4205, 2023. 3

[27] Robin Rombach, Andreas Blattmann, Dominik Lorenz, Patrick Esser, and Björn Ommer. High-resolution image synthesis with latent diffusion models. In *Proceedings of the IEEE/CVF conference on computer vision and pattern recognition*, pages 10684–10695, 2022. 3

[28] Ethan Rublee, Vincent Rabaud, Kurt Konolige, and Gary Bradski. Orb: An efficient alternative to sift or surf. In *2011 International conference on computer vision*, pages 2564–2571. Ieee, 2011. 2, 5

[29] Jiaming Song, Chenlin Meng, and Stefano Ermon. Denoising diffusion implicit models. *arXiv preprint arXiv:2010.02502*, 2020. 3

[30] Peize Sun, Yi Jiang, Shoufa Chen, Shilong Zhang, Bingyue Peng, Ping Luo, and Zehuan Yuan. Autoregressive model beats diffusion: Llama for scalable image generation. *arXiv preprint arXiv:2406.06525*, 2024. 3

[31] Meituan LongCat Team, Xunliang Cai, Qilong Huang, Zhuoliang Kang, Hongyu Li, Shijun Liang, Liya Ma, Siyu Ren, Xiaoming Wei, Rixu Xie, et al. Longcat-video technical report. *arXiv preprint arXiv:2510.22200*, 2025. 3

[32] Hansi Teng, Hongyu Jia, Lei Sun, Lingzhi Li, Maolin Li, Mingqiu Tang, Shuai Han, Tianning Zhang, WQ Zhang, Weifeng Luo, et al. Magi-1: Autoregressive video generation at scale. *arXiv preprint arXiv:2505.13211*, 2025. 2, 3

[33] Keyu Tian, Yi Jiang, Zehuan Yuan, Bingyue Peng, and Liwei Wang. Visual autoregressive modeling: Scalable image generation via next-scale prediction. *Advances in neural information processing systems*, 37:84839–84865, 2024. 3

[34] Team Wan, Ang Wang, Baole Ai, Bin Wen, Chaojie Mao, Chen-Wei Xie, Di Chen, Feiwu Yu, Haiming Zhao, Jianxiao Yang, et al. Wan: Open and advanced large-scale video generative models. *arXiv preprint arXiv:2503.20314*, 2025. 2, 3

[35] Yuqing Wang, Tianwei Xiong, Daquan Zhou, Zhijie Lin, Yang Zhao, Bingyi Kang, Jiashi Feng, and Xihui Liu. Loong: Generating minute-level long videos with autoregressive language models. *arXiv preprint arXiv:2410.02757*, 2024. 3

[36] Yaohui Wang, Xinyuan Chen, Xin Ma, Shangchen Zhou, Ziqi Huang, Yi Wang, Ceyuan Yang, Yinan He, Jiashuo Yu, Peiqing Yang, et al. Lavie: High-quality video generation with cascaded latent diffusion models. *International Journal of Computer Vision*, 133(5):3059–3078, 2025. 2, 3

[37] Zeqi Xiao, Yushi Lan, Yifan Zhou, Wenqi Ouyang, Shuai Yang, Yanhong Zeng, and Xingang Pan. Worldmem: Long-term consistent world simulation with memory. *arXiv preprint arXiv:2504.12369*, 2025. 2, 3

[38] Mengjiao Yang, Yilun Du, Kamyar Ghasemipour, Jonathan Tompson, Dale Schuurmans, and Pieter Abbeel. Learning interactive real-world simulators. *arXiv preprint arXiv:2310.06114*, 1(2):6, 2023. 3

[39] Zhuoyi Yang, Jiayan Teng, Wendi Zheng, Ming Ding, Shiyu Huang, Jiazheng Xu, Yuanming Yang, Wenyi Hong, Xiaohan Zhang, Guanyu Feng, et al. Cogvideox: Text-to-video diffusion models with an expert transformer. *arXiv preprint arXiv:2408.06072*, 2024. 3

[40] Tianwei Yin, Qiang Zhang, Richard Zhang, William T Freeman, Fredo Durand, Eli Shechtman, and Xun Huang. From slow bidirectional to fast autoregressive video diffusion models. In *Proceedings of the Computer Vision and Pattern Recognition Conference*, pages 22963–22974, 2025. 3

[41] Jiwen Yu, Jianhong Bai, Yiran Qin, Quande Liu, Xintao Wang, Pengfei Wan, Di Zhang, and Xihui Liu. Context as memory: Scene-consistent interactive long video generation with memory retrieval. *arXiv preprint arXiv:2506.03141*, 2025. 2, 3

[42] Jiwen Yu, Yiran Qin, Xintao Wang, Pengfei Wan, Di Zhang, and Xihui Liu. Gamefactory: Creating new games with generative interactive videos. *arXiv preprint arXiv:2501.08325*, 2025. 3

[43] Lijun Yu, José Lezama, Nitesh B Gundavarapu, Luca Verhari, Kihyuk Sohn, David Minnen, Yong Cheng, Vighnesh Birodkar, Agrim Gupta, Xiuye Gu, et al. Language model beats diffusion–tokenizer is key to visual generation. *arXiv preprint arXiv:2310.05737*, 2023. 3

[44] Lvmin Zhang and Maneesh Agrawala. Packing input frame context in next-frame prediction models for video generation. *arXiv preprint arXiv:2504.12626*, 2025. 3

[45] Yifan Zhang, Chunli Peng, Boyang Wang, Puyi Wang, Qingcheng Zhu, Fei Kang, Biao Jiang, Zedong Gao, Eric Li, Yang Liu, et al. Matrix-game: Interactive world foundation model. *arXiv preprint arXiv:2506.18701*, 2025. 2, 3

[46] Zangwei Zheng, Xiangyu Peng, Tianji Yang, Chenhui Shen, Shenggui Li, Hongxin Liu, Yukun Zhou, Tianyi Li, and Yang You. Open-sora: Democratizing efficient video production for all. *arXiv preprint arXiv:2412.20404*, 2024. 3

[47] Chunting Zhou, Lili Yu, Arun Babu, Kushal Tirumala, Michihiro Yasunaga, Leonid Shamis, Jacob Kahn, Xuezhe Ma, Luke Zettlemoyer, and Omer Levy. Transfusion: Predict the next token and diffuse images with one multi-modal model. *arXiv preprint arXiv:2408.11039*, 2024. 3

StableWorld: Towards Stable and Consistent Long Interactive Video Generation

Supplementary Material

Appendix

A. Algorithmic Implementation

Algorithm 1: Dynamic Frame Eviction via ORB-based Geometric Similarity

Input: Sliding window $\{L_0, \dots, L_{N-1}\}$ in latent space; pixel frames $\{P_0, \dots, P_{N-1}\}$, earlier frames in the window $\{P_0, P_1, \dots, P_K\}$ with $K < N - 1$; similarity threshold θ .

Output: Updated window after eviction.

Extract ORB features from the reference frame P_0 .

for $k = 1$ **to** K **do**

- Extract ORB features from the current frame P_k .
- Compute descriptor matches

 - $G = \{(i, j) \mid \|d_i^{(0)} - d_j^{(k)}\| < \tau\}$.

- Estimate Homography \mathbf{H} and Fundamental matrix \mathbf{F} via RANSAC.
- Compute inlier ratios $r_H = \frac{|\mathcal{I}_H|}{|G|}$, $r_F = \frac{|\mathcal{I}_F|}{|G|}$, and define similarity $s(P_0, P_k) = \max(r_H, r_F)$.
- if** $s(P_0, P_k) < \theta$ **then**

 - break**

Evict the farthest latent frame P_{k-1} from the window.

Insert the newly generated frame to maintain window size N .

In practice, we implement the geometric similarity computation in Algorithm 1 using an ORB-based matching procedure. For each frame pair (P_0, P_k) , up to 3000 ORB keypoints are extracted with OpenCV’s `ORB_create` (FAST threshold = 7). Descriptor matching is performed using a brute-force matcher with Hamming distance and a two-nearest-neighbor ratio test. The ratio threshold τ is set to 0.8 following Lowe’s criterion, and the resulting good matches are further filtered by RANSAC using both the Homography \mathbf{H} and Fundamental matrix \mathbf{F} models. The RANSAC reprojection tolerance ϵ is fixed to 3.0 pixels, and the confidence level is set to 0.99 for Fundamental-matrix estimation. The inlier ratios r_H and r_F are computed as the proportions of the inlier correspondence sets \mathcal{I}_H and \mathcal{I}_F over all valid matches, and the final similarity score $s(P_0, P_k)$ is defined as $\max(r_H, r_F)$. Frames with fewer than five valid correspondences are considered unreliable and assigned a similarity score of 0. We empirically set the eviction threshold θ to 0.75 in all experiments.

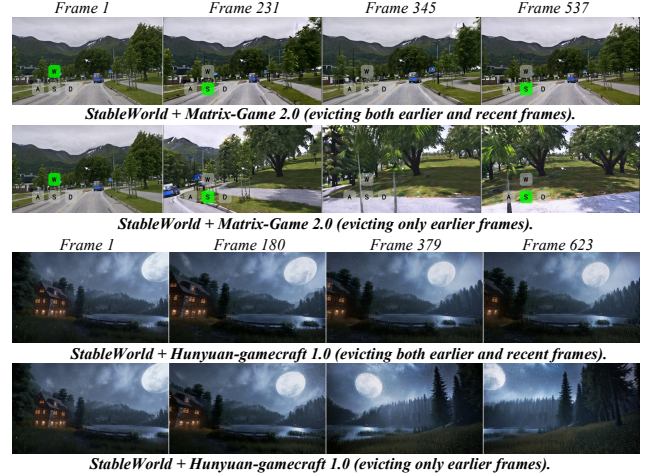


Figure 13. Comparison between evicting both earlier and recent frames and evicting only earlier frames in *StableWorld*.

B. Additional Ablation

Length of Frames Evicted in the Window. We further investigate the effect of evicting both earlier frames and recent frames, as illustrated in Fig. 13. All settings are tested under identical action conditions for fair comparison. As shown in the figure, evicting recent frames leads to inconsistent motion and unstable short-term dynamics, which in turn hinders the generation of subsequent frames. This behavior is analogous to retaining too many frames in the window: both strategies reduce the model’s adaptability to scene changes and limit its ability to transition smoothly to new environments. In contrast, selectively removing earlier degraded frames preserves local motion continuity while maintaining sufficient flexibility for handling scene transitions.

C. More Qualitative Results

We present additional qualitative results for *Matrix-Game 2.0* in Fig. 16. From these more diverse outputs, we observe that *StableWorld* significantly strengthens stability during long-horizon generation. We further evaluate *StableWorld* on extremely long frame sequences (e.g., thousands of frames) under both small-motion settings (Fig. 17) and large-motion scenarios (Fig. 18). More Qualitative comparisons on *Open-Oasis* and *Hunyuan-GameCraft 1.0* are provided in Fig. 19 and Fig. 20, respectively. Across all settings, we observe that our method effectively prevents cumulative errors by continuously filtering out degraded frames while maintaining coherent motion. As a result, *StableWorld* produces notably more stable and temporally consistent interactive



A girl rapidly teleports from a cozy **living room** to a deep **forest**, then to a **rainy alley**, then to a sunny rooftop, and finally to a desert **highway**. Each scene switch is sudden and dramatic.



A man instantly switches between environments: sitting in a **café**, walking through a **shopping mall**, standing on a **windy hilltop**, appearing inside a **futuristic laboratory**, and then on a busy **street** at night.

Figure 14. Qualitative results of *Self-Forcing* in a fast-changing scene. When the scene changes frequently, the model shows fewer cases of scene collapse, although the visuals may still appear inconsistent across frames.

video sequences.

D. Qualitative Results in Autoregressive Video Generation

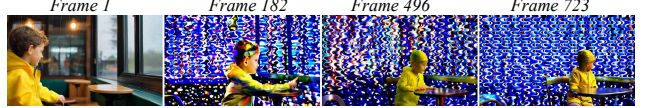
We further validate the effectiveness of *StableWorld* in long-horizon autoregressive video generation. We use the *Self-Forcing* model as our baseline.

We also observe that *Self-Forcing* exhibits the same phenomenon as in the interactive video generation setting. As shown in Fig. 14, when the scene changes frequently, catastrophic collapse rarely occurs. In contrast, in Fig. 15, where the model stays within the same scene and the changes are relatively small, collapse emerges clearly: small inter-frame drift gradually accumulates within the same scene and eventually leads to severe degradation. This confirms that error accumulation in autoregressive generation is closely linked to drift propagation within a persistent scene.

We then integrate our method into the *Self-Forcing* framework. We set the key-value cache length to 9 and treat the earliest 6 frames as reference frames. Since the model produces 3 frames per step, we compute the ORB-based geometric similarity between the 3rd and 6th frames to decide whether the earliest frames should be evicted. A qualitative comparison is shown in Fig. 21. As can be seen, *StableWorld* significantly alleviates error accumulation in *Self-Forcing*, resulting in more stable, consistent, and higher-quality long videos. These results demonstrate that our approach offers a promising solution for mitigating drift in long-term autoregressive video generation.

E. Limitation

One limitation of our method is the slight increase in inference time introduced by the computation of ORB-based geometric similarity, resulting in approximately a $1.01\times$ –



A boy in a raincoat enters a small **café**, shakes the raindrops off his hood, and chooses a seat near the window.



A man sits at a wooden desk in a quiet **study**, hands folded, gazing gently out the window.

Figure 15. Qualitative results of *Self-Forcing* in a low-motion scene. Even with minimal scene changes, *Self-Forcing* exhibits noticeable drift accumulation that eventually leads to scene collapse.

$1.02\times$ slowdown compared with the vanilla model under the default setting. However, we believe this enables the sliding-window length to become dynamically adjustable by discarding drifted frames, thereby reducing its associated computational cost, which in turn lowers the overall inference time. We leave this direction for future exploration.

F. Future Work.

In future work, we plan to explore integrating *StableWorld* into the training process to further extend the length and stability of interactive video generation. Moreover, the ability to identify and discard a large number of drifted frames during generation has the potential to reduce training cost and aligns naturally with future extensions toward memory-augmented world models.

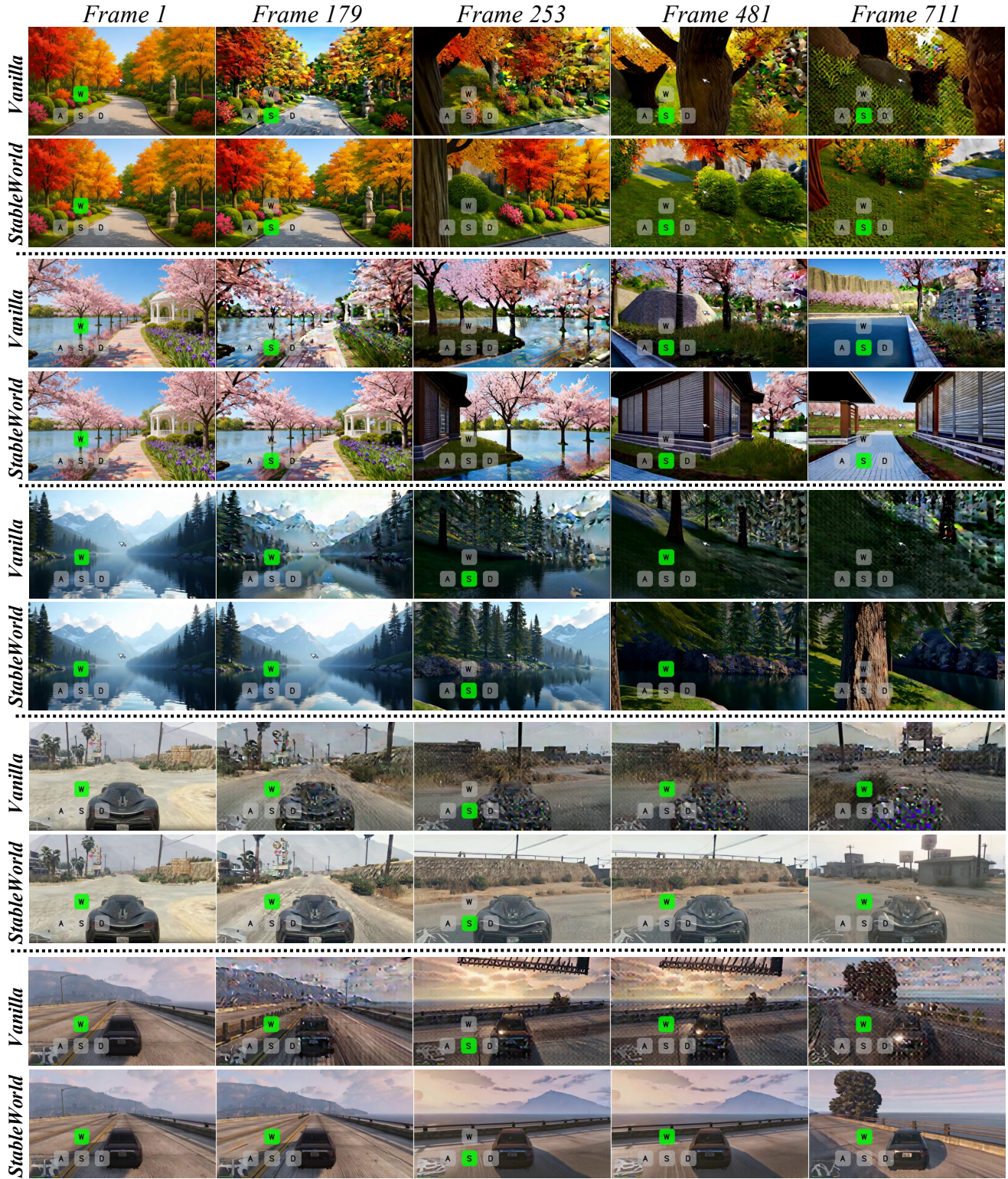


Figure 16. Additional qualitative comparison between *Matrix-Game 2.0* and our *StableWorld*. The first row shows *Matrix-Game 2.0*; the second row shows *StableWorld*. *StableWorld* shows more stable results with better visual quality.



Figure 17. Long-horizon generation results of *StableWorld* under small-motion scenarios. The model maintains scene stability over thousands of frames without drift or degradation.



Figure 18. Long-horizon generation results of *StableWorld* under large-motion scenarios. Despite significant viewpoint and motion changes, *StableWorld* preserves temporal consistency and avoids cumulative drift.

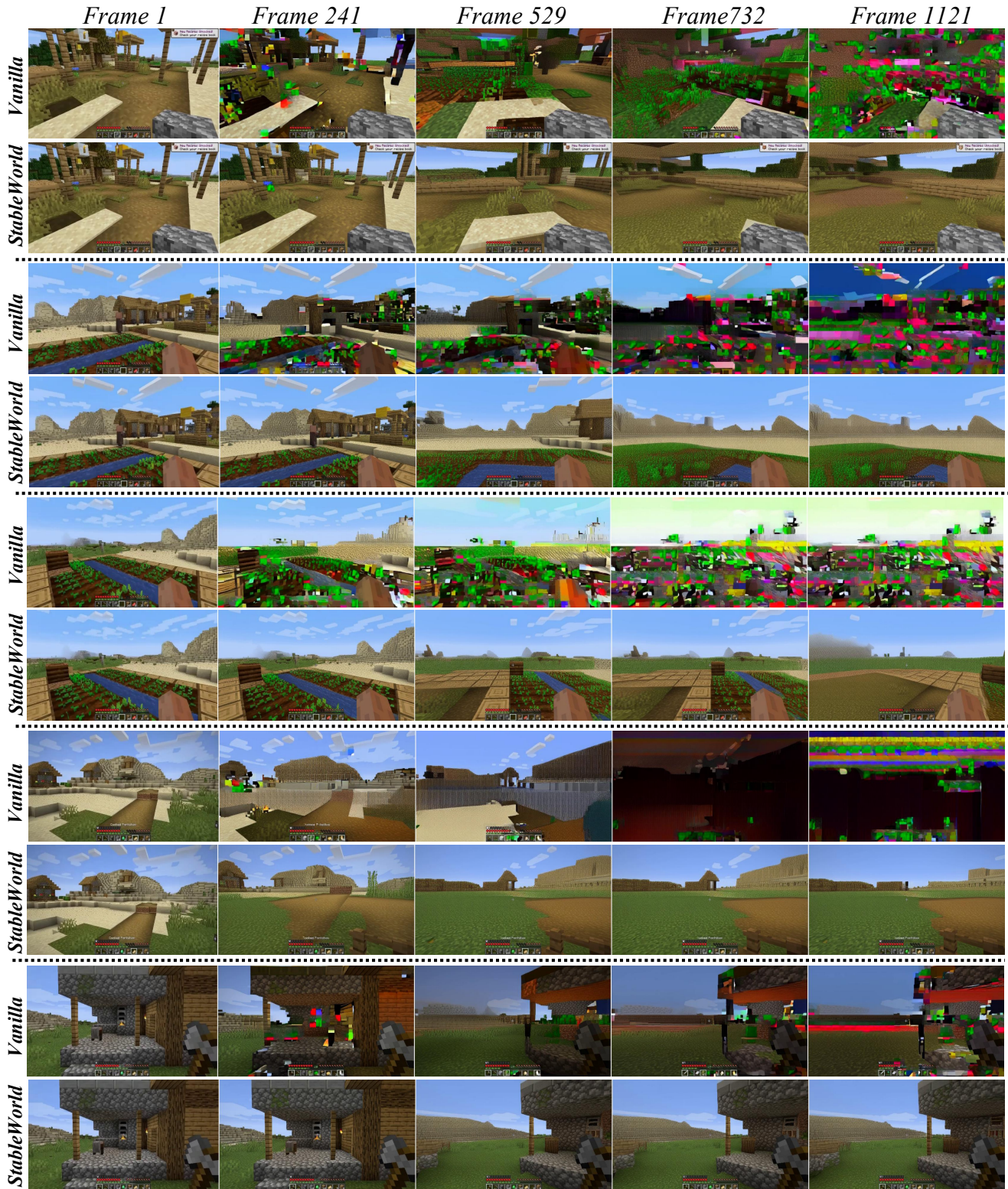


Figure 19. Additional qualitative comparison between *Open-Oasis* and our *StableWorld*. The first row shows *Open-Oasis*; the second row shows *StableWorld*. *StableWorld* shows more stable results with better visual quality.



Figure 20. Additional qualitative comparison between *Hunyuan-GameCraft 1.0* and our *StableWorld*. The first row shows *Hunyuan-GameCraft 1.0*; the second row shows *StableWorld*. *StableWorld* shows more stable results with better visual quality.

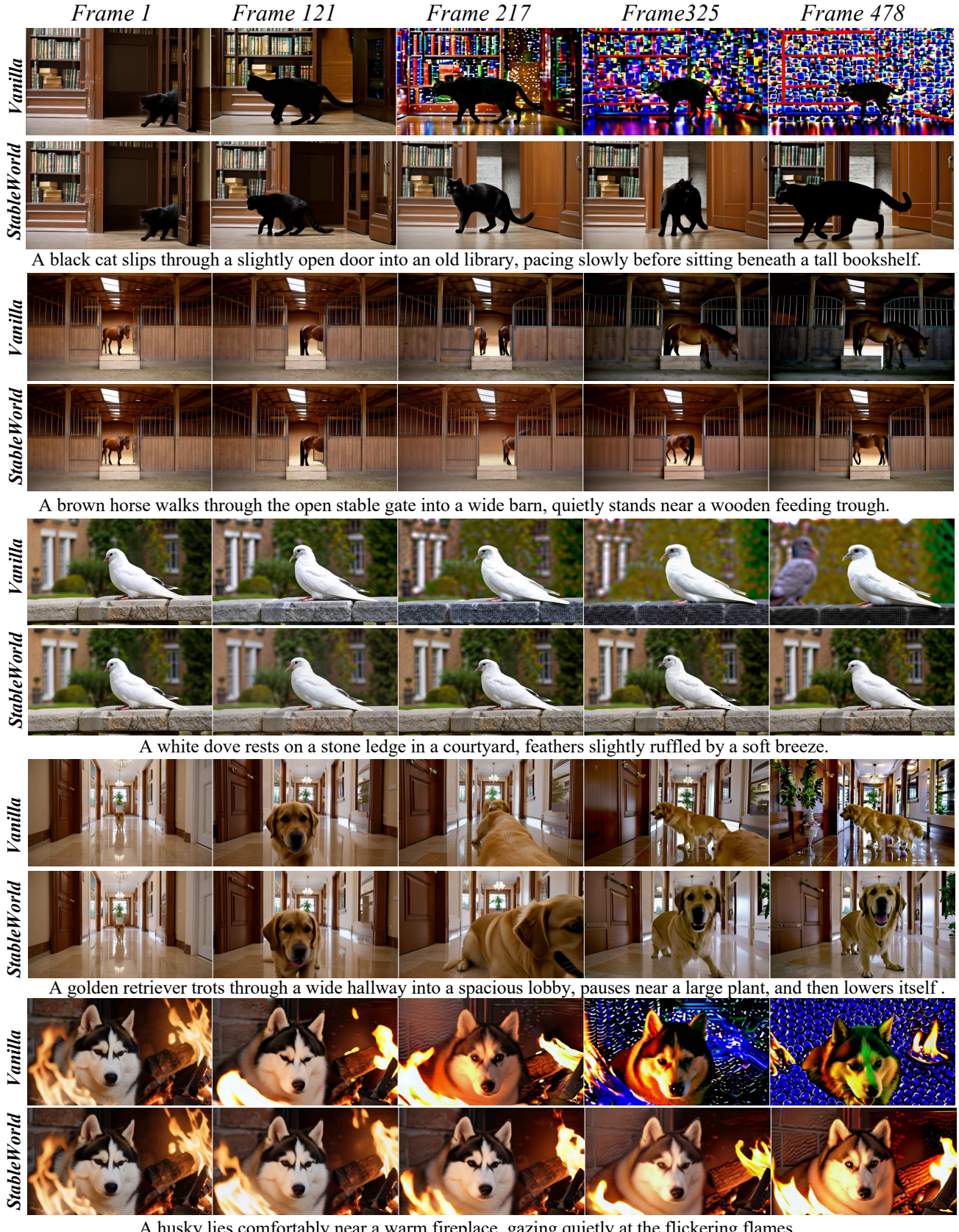


Figure 21. Additional qualitative comparison between *self-forcing* and our *StableWorld*. *StableWorld* shows more stable results with better visual quality.